Dalton Transactions

ROYAL SOCIETY OF CHEMISTRY

PAPER

View Article Online
View Journal | View Issue

Open Access Article. Published on 06 February 2020. Downloaded on 12/7/2025 11:21:56 AM.
This article is licensed under a Creative Commons Attribution-NonCommercial 3.0 Unported Licence.

Cite this: *Dalton Trans.*, 2020, **49**, 2706

2,5-Bis-trimethylsilyl substituted boroles†

Tobias Heitkemper, Leonard Naß and Christian P. Sindlinger *

This manuscript includes a comprehensive study of the synthesis and spectroscopic features of 2,5-disilyl boroles. Reacting boron trichloride BCl_3 with 2,3-Ph*$_2$-1,4-(SiMe$_3$)$_2$-1,4-dilithiobuta-1,3-diene (Ph* = 3,5-*t*-Bu$_2$(C$_6$H$_3$)) allowed reliable access to 1-Chloro-2,5-(SiMe$_3$)$_2$-3,4-(Ph*)$_2$-borole in good yields (60%). Unlike 2,3,4,5-tetraphenyl haloboroles, this 2,5-bis-trimethylsilyl substituted chloroborole is thermally stable in solution to up to 130 °C. Metathesis reactions of the chloroborole with metal aryls or of the dilithiobutadiene with arylboron dihalides grant access to 1-Ar-2,5-(SiMe$_3$)$_2$-3,4-(Ph*)$_2$ boroles (Ar = Ph, Mes, Ph*, C$_6$F$_5$). Unlike the generally intensely blue-green 2,3,4,5-tetraaryl boroles, brightly orange/red 2,5-bis-trimethylsilyl substituted boroles reveal blue-shifted π/π*-transitions due to a lack of π-system interaction between borole and 2,5-bound aryls. Light is shed on the synthetic peculiarities for the synthesis of 2,5-disilyl-boroles. While direct treatment of the respective 1,1-dimethyl-stannole with $ArBCl_2$ *via* otherwise well-established B/Sn exchange reactions fails, the selectivity of reactions of 2,3-Ph*$_2$-1,4-(SiMe$_3$)$_2$-1,4-dilithiobuta-1,3-diene with $ArBCl_2$ is solvent dependent and leads to rearranged 3-borolenes in hydrocarbons. Gutmann–Beckett analysis reveal reduced Lewis-acidity of disilylboroles compared to pentaphenyl borole.

Received 13th January 2020,
Accepted 3rd February 2020

DOI: 10.1039/d0dt00393j

rsc.li/dalton

Introduction

Among unsaturated five-membered main group heterocycles, 1*H*-boroles adopt a unique position. Isoelectronic to the elusive cyclopentadienyl cation, with four π-electrons in cyclic conjugation *via* the empty p-orbital of boron, these systems exhibit a weakly *anti*-aromatic character.[1–6] Free boroles are very reactive species that add dihydrogen or silane Si–H bonds across the π-system,[7–10] react as potent Lewis-acids also towards weak bases,[2,11–13] engage in various Diels–Alder and ring-expansion reactions[14–31] or readily accept two electrons to form dianionic 6π-electron systems.[32–35] Boroledиides are isoelectronic to cyclopentadienyl anions and have thus been used and studied as ligands in transition metal coordination chemistry.[32,36–46] Only recently accounts of boroles as π-ligands for p-block elements (Al, Ge) have been reported.[47,48] Bearing rather small substituents, free boroles undergo Diels–Alder dimerization. These dimers can provide a source of monomeric borole synthons upon thermal treatment.[49–51]

With free boroles being so reactive, to date, their synthesis and successful isolation is limited to relatively few substituents around the central C_4B cycle.[52] Most reports on free borole chemistry discuss pentaaryl boroles[34,53,54] and particularly $(PhC)_4BAr$ for which reliable synthetic protocols exist. Here, a key reaction involves the commercially available diphenyl acetylene which can be readily reductively coupled with lithium to provide 1,4-dilithiobuta-1,3-dienes as valuable precursor for further derivatization.[5,6] This allowed for the synthesis of tetraphenylboroles with varying boron-bound substituents in the past.[2,33,55–60]

The 2,5-bis-trimethylsilyl-butadiene backbone has recently found application for s-/ and p-block element metaloles, mainly driven by the groups of Xi (groups 2 and 13), Saito and Müller (group 14).[61–81] However, only very few examples of 2,5-bis-trialkylsilyl-substituted boroles are known, all of which have been accessed *via* synthetically rather unusual routes (Scheme 1). Saito and coworkers obtained free fluoroborole **A** *via* Pb/B exchange reactions starting from donor-stabilized plumbole.[69] Erker and coworkers reported formation of free 2,5-bis-trimethylsilyl boroles **B** by 1,1-carboborations after treatment of bis-alkynylboranes with tris(pentafluorophenyl) borane BPh^F_3.[82] Other than these free boroles, the borole motive can be found in Sekiguchi's and Lee's dilithio boroledиide obtained from reduction of chloro borapyramidane as well as Müller's and Albers' Ge(II) complex of a boroledиide.[47,83]

We are eager to extend the library of accessible free boroles with regards to the substituents attached to boron and carbon atoms of the central moiety and to study the electronic

Institut für Anorganische Chemie, Tammannstr. 4, 37077 Göttingen, Germany. E-mail: christian.sindlinger@chemie.uni-goettingen.de

†Electronic supplementary information (ESI) available: Experimental and synthetic details, depiction of spectra and crystal structures, computational details. CCDC 1976852–1976861. For ESI and crystallographic data in CIF or other electronic format see DOI: 10.1039/d0dt00393j

This journal is © The Royal Society of Chemistry 2020

Open Access Article. Published on 06 February 2020. Downloaded on 12/7/2025 11:21:56 AM.
This article is licensed under a Creative Commons Attribution-NonCommercial 3.0 Unported Licence.

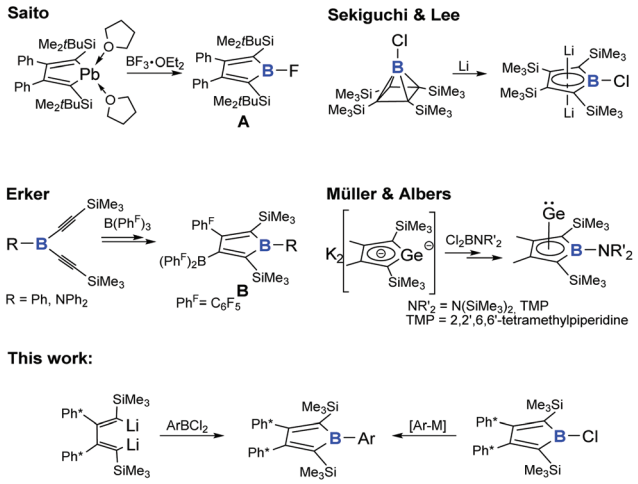

Scheme 1 Examples of 2,5-disilyl-boroles.

impacts of each individual substituent.[84] Here we report on the synthetic access to 2,5-bis-trimethylsilyl substituted boroles.

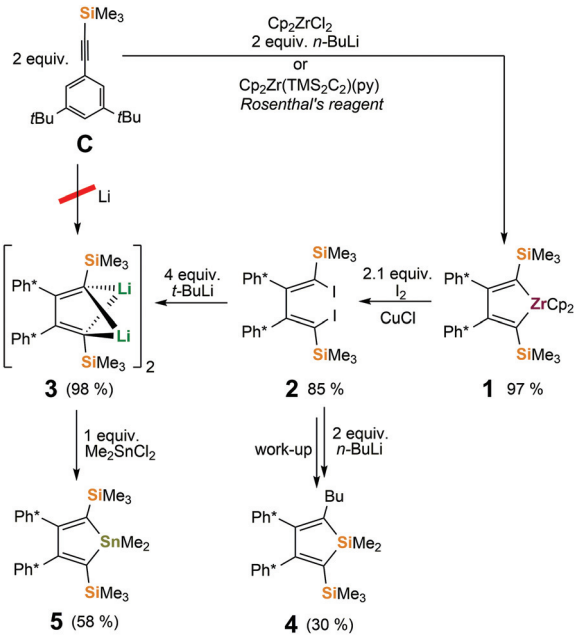

Scheme 2 Precursor syntheses.

Results and discussion

Precursor synthesis

Free boroles $(RC)_4BR'$ are usually accessed *via* salt metathesis reaction of 1,4-dilithiobuta-1,3-dienes or B/Sn exchange reactions of the respective stannole with boron dihalides RBX_2. Stannoles are again either obtained from 1,4-dilithiobuta-1,3-dienes or Fagan–Nugent-type Sn/Zr transmetallations from the respective zirconacyclopentadiene.[85–87] 1,4-Dilithiobuta-1,3-dienes are accessed by reductive coupling of acetylenes with lithium or from 1,4-diiodobuta-1,3-dienes. The latter are generally derived from zirconacyclopentadienes. However, access to any of these (cyclic) 1,4-dimetalla-1,3-butadiene precursors strongly depends on the nature of the substituents. Especially coupling of silylacetylenes over lithium is heavily depending on the substituents.[88]

We are keen to provide systems that are soluble in apolar hydrocarbon solvents and therefore anticipated 3,5-di-*t*-butylphenyl-trimethylsilyl acetylene **C** Ph*CCSiMe$_3$ (Ph* = 3,5-*t*-Bu$_2$(C$_6$H$_3$)) to be a suitable building block to start from. Acetylene **C** however did not reveal any reaction with lithium metal and thus we had to take the detour *via* established zirconacyclopentadiene protocols using Negishi's or Rosenthal's reagents.[89,90] 2,5-Disilyl-zirconacyclopentadiene **1** forms in excellent yields (>95%) (Scheme 2). However, likely due to steric pressure of the substituents **1** reversibly eliminates alkyne over time (see ESI†).[91] Our attempts for direct Zr/Sn transmetallation of **1** with Me_2SnCl_2 to stannole **5** failed (see ESI†). Reactions of **1** with boron halides $RBCl_2$ neither produced boroles **6** or boryl-borolenes **7** (*vide infra*) but led to formation of yet unidentified products.

CuCl-supported iodination of *in situ* generated zirconacyclopentadiene **1** reliably yields the anticipated (*Z*,*Z*)-isomer of 1,4-diiodo-butadiene **2**.[92] In our hands, iodination of previously isolated **1** has under identical conditions led to unfavourable mixtures of (*Z*,*Z*) and (*E*,*Z*)-isomers of **2** (see ESI†). **2** is conveniently transformed into the 1,4-dilithiobuta-1,3-diene **3** with *tert*-butyllithium in essentially quantitative yield (98%). 1,4-Dilithiobuta-1,3-diene **3** is obtained as an intensely orange crystalline solid which revealed a dimeric structure in the solid state (Fig. 1). The central distorted [Li$_4$]-tetrahedron reveals its longest Li–Li distances between Li-atoms that are connected to

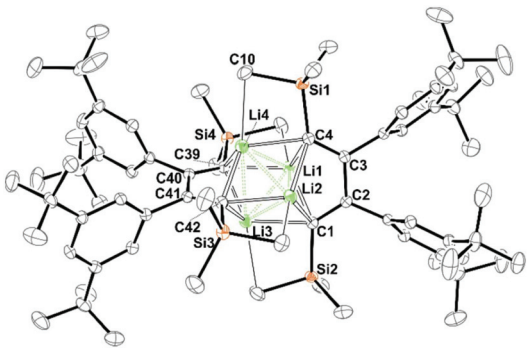

Fig. 1 ORTEP plot of the solid-state structure of dimeric 1,4-dilithiobuta-1,3-diene (**3**)$_2$. Anisotropic displacement parameters are drawn at 50% probability level. Selected bond length [Å] are given: Li1–C1 2.105(3), C1–Li2 2.173(3), Li1–C4 2.169(3), Li1–C39 2.198(3), Li2–C4 2.112(3), Li2–C42 2.214(3), Li3–C39 2.114(3), Li3–C42 2.170(3), Li4–C42 2.100(3), Li4–C39 2.165(3), Li4–C4 2.195(3), C1–Li3 2.215(3), Li1–Li2 2.721(3), Li1–Li3 2.390(3), Li1–Li4 2.496(3), Li2–Li4 2.386(3), Li2–Li3 2.482(3), Li3–Li4 2.696(3), C1–C2 1.365(2), C2–C3 1.542(2), C3–C4 1.368(2), C39–C40 1.366(2), C40–C41 1.538(2), C41–C42 1.367(2), Li4–C10 2.423(3).

Open Access Article. Published on 06 February 2020. Downloaded on 12/7/2025 11:21:56 AM.
This article is licensed under a Creative Commons Attribution-NonCommercial 3.0 Unported Licence.

the same butadiene dianion. All lithium atoms feature a further short contact (Li–C_{TMS} 2.423(3)–2.472(3)) to one silicon-bound methyl group thus also providing steric protection of the reactive nucleus. A related structure was previously reported by Saito and coworkers.[88]

When Li/I exchange was attempted applying *n*-butyllithium followed by subsequent quenching of *in situ* generated **3** with Me_2SnCl_2 at 0 °C, rearrangements were observed to take place and we isolated and identified silole **4** as a major product.[93] Under these conditions, butyl iodide apparently reacts with dilithio-butadiene **3**. Thus, using *t*-BuLi to produce **3** remained the more reliable approach. In the presence of HMPA (OP$(NMe_2)_3$), formation of 1,1-dimethylsiloles from rearrangements of 1,4-dilithio-1,4-disilylbuta-1,3-dienes, presumably *via* 2-lithiosilole and MeLi elimination, was described earlier by Xi and coworkers.[94,95]

Reaction of **3** with a mild electrophile such as Me_2SnCl_2 yielded the 1,1-dimethylstannole **5** in moderate crystalline yields (58%).[71,96] Unfortunately however, the well-established boron-tin exchange reaction with arylboron dichlorides $RBCl_2$ (R = Ph, Xyl^F {Xyl^F = 3,5-$(CF_3)_2(C_6H_3)$}), that allows convenient and clean access to boroles with 2,3,4,5-tetraaryl-butadiene backbones[5,33,84] does not occur in the case of this 2,5-disilyl system (Scheme 3). No formation of Me_2SnCl_2 is observed in NMR screening reactions. Side reactions leading to intractable product mixtures likely involve methyl abstraction from the tin atom in **5**. An abnormal B/Sn exchange reaction behaviour was recently reported by Braunschweig and coworkers.[97]

Being short of one major synthetic pathway to boroles, we thus turned to direct treatment of 1,4-dilithiobutadiene **3** with organoboron dihalides. Reactions of **3** and 1 equiv. of $ArBCl_2$ in THF revealed to cleanly (>90% by NMR) form the aryl boroles and allowed isolation of **6-Ph** and **6-Ph*** in good yields (Scheme 4). However, quantitative removal of THF from the resulting Lewis-acidic boroles *in vacuo* (10^{-3} mbar) for several days was found to be tedious. The application of THF is therefore usually avoided when free boroles are targeted. While **6-Ph*** was obtained free of donor solvent after drying *in vacuo*, **6-Ph** always contained residual amounts of THF, despite their Lewis-acidities were found to be identical (Gutmann–Beckett method, see below). At mildly elevated temperatures (40 °C) THF is liberated from **6-Ph**, however substantial decomposition occurs.

With $MesBCl_2$ the THF route fails completely. In Et_2O, borole formation from **3** with $ArBCl_2$ was much less selective and did not provide satisfyingly pure material. However, when **3** was analogously reacted with phenylboron dichloride in

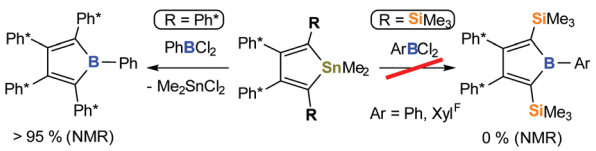

Scheme 3 Attempted boron-tin-exchange Reactions.

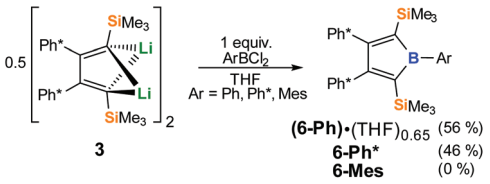

Scheme 4 Reaction of **3** towards boron electrophiles in THF (yields after crystallisation).

hexane or benzene in order to access free organoboroles, irrespective of the applied stoichiometric ratio of the reagents, a clean consumption of 2 equiv. $PhBCl_2$ per **3** took place yielding a 2-borylated 3-borolene **7-Ph**. The structure of racemic mixtures of **7-Ph** is confirmed by an X-ray structure (Fig. 2) and reveals a double bond between C2 and C3. We reason, that formation of **7-Ph** involves the intermediate generation of the anticipated phenyl–borole and rapid subsequent addition of a second equivalent of $PhBCl_2$ *via* an electrophilic attack of $PhBCl_2$ at one C_α atom in the borole (Scheme 5).

These C_α positions should be considerably nucleophilic given they bear two electropositive atom substituents (–$SiMe_3$ and –BR_2) and the Si β-effect should further moderate the α-addition of the B-electrophile in these special cases of vinylsilanes. Within the rearrangement sequence, the B-bound Ph-residue then migrates to the other C_α when a chloride adds to the borole B-atom. The addition of a second equivalent $ArBCl_2$ to **6-Ar** is facilitated by the removal of *anti*-aromatic cyclic 4π-electron delocalization and stabilizing lonepair π-donation from Cl into the empty p-orbital of boron. Addition of B–H moieties across a borole to give 2-boryl-3-borolenes where reported earlier.[10] Somewhat related chemistry was described for the reaction of azobenzene with $(PhC)_4BPh$.[98] Similar reaction behavior consuming 2 equiv. of aryl boron dihalides per **3** are also observed for the reactions with $ArBCl_2$ (Ar = Ph*, Xyl^F).

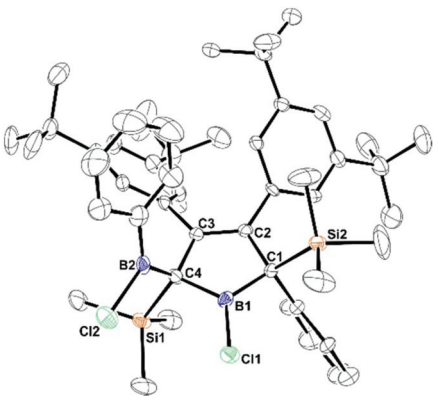

Fig. 2 (a) ORTEP plot of the solid-state structure of 2-boryl-3-borolene (**7-Ph**). Anisotropic displacement parameters are drawn at 50% probability level. Only one moleculare within the asymmetric unit is shown. Selected bond length [Å] are given: B1–Cl1 1.766(4), B1–C1 1.569(6), C1–C2 1.533(5), C2–C3 1.353(6), C3–C4 1.545(5), B1–C4 1.586(6), C4–B2 1.553(5), B2–Cl2 1.814(4).

This journal is © The Royal Society of Chemistry 2020

Open Access Article. Published on 06 February 2020. Downloaded on 12/7/2025 11:21:56 AM.
This article is licensed under a Creative Commons Attribution-NonCommercial 3.0 Unported Licence.

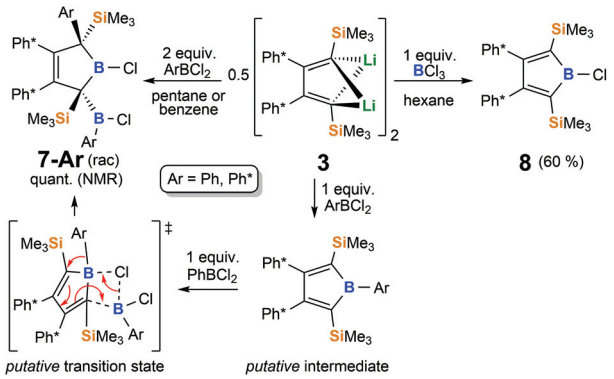

Scheme 5 Reaction of **3** towards boron electrophiles in hydrocarbons.

To support the proposed mechanism *via* formation of the free borole, 1 equiv. of isolated free borole **6-Ph*** was treated with the respective Ph*BCl_2 to give the same asymmetric compound 2-boryl-3-borolene **7-Ph*** as the reaction of **3** with 2 equiv. of Ph*BCl_2, thus corroborating the proposed mechanism (see ESI†). Notably, with Ar = Mes (Mes = 2,4,6-$Me_3(C_6H_2)$, no reaction occurred at all, while $(PhC)_4$BMes is reported to be readily formed from $(PhC)_4Li_2$ and $MesBCl_2$.[58] Also when the electrophilicity of the boron species is reduced such as in *i*-Pr_2NBCl_2 or in the Lewis-adduct $PhBCl_2$(DMAP) (DMAP = 4-(*N*′,*N*′-dimethylamino)pyridine), dilithio-butadiene **3** did not reveal any reaction in C_6H_6 or Et_2O.

To our surprise, when a solution of **3** was treated with 1 equiv. of boron trichloride in hexane, chloroborole **8** was isolated in moderate yields of about 60% as an orange-red crystalline solid. Unlike in the previously discussed reactions of arylboron dihalides, feasibility of the isolation of **8** likely stems from stabilizing np-π-donation interactions reducing both the Lewis-acidity and *anti*-aromatic character of chloroborole **8**. An X-ray crystallographic examination revealed the structure of **8** as only the third example of a crystallographically characterized haloborole (Fig. 3).

Bond lengths within the C_4B-ring are essentially identical to fluoroborole **A** (Scheme 1) and $(PhC)_4$B–Cl with the B1–Cl1 bond of 1.7543(17) Å in **8** being slightly longer than in the latter (1.7433(13) Å).[55] Unlike for these other haloboroles, the substituents around the central C_4B-ring slightly bend out of the least-square plane through the borole atoms (Fig. 3b). While substituents at C4 and C3 essentially lie within the plane, substituents at B1, C1 and C2 alternatingly bend out above or below the central plane by *ca.* 11(1)° each.

The amount of known 1-haloboroles in total is limited to four stable examples. Eisch's and Braunschweig's previously reported 2,3,4,5-tetraphenyl-haloboroles either dimerize at 40 °C ($(PhC)_4$B–Cl)[55] or 55 °C ($(PhC)_4$B–Br)[57] or even decompose at ambient temperature over time. Marder reported on a transient chloroborole that readily dimerizes.[99] This 2,5-disilyl chloroborole **8** is remarkably thermally stable and even forcing conditions in benzene at 130 °C (in a Teflon-valve sealed NMR-tube) for several hours did not indicate any decomposition

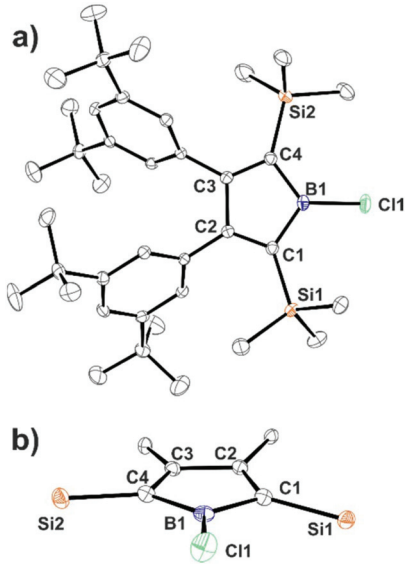

Fig. 3 (a) ORTEP plot of the solid-state structure of chloroborole (**8**). Anisotropic displacement parameters are drawn at 50% probability level. (b) Excerpt of the central substituted C_4B-ring. Selected bond length [Å] are given: B1–Cl1 1.7543(17), B1–C1 1.564(2), C1–C2 1.354(2), C2–C3 1.538(2), C3–C4 1.353(2), B1–C4 1.568(2), C1–Si1 1.8683(15), Si2–C4 1.8725(16).

of **8**. Its thermal stability thus more resembles Piers' perfluorinated 2,3,4,5-tetraphenyl bromoborole $(Ph^FC)_4$B–Br (Ph^F = (C_6F_5)).[54] Stable haloboroles are key synthetic precursors to borolyl-substituted systems. By functionalization of $(PhC)_4$BCl, Braunschweig and coworkers previously accessed aminoboroles or even oxidatively added the B–Cl bond across the zero-valent metal in $[Pt(PCy_3)_2]$.[2,56]

The ^{11}B-NMR signal of **8** is found as a broad resonance ($\omega_{1/2}$ = 1370 Hz) at δ_{11B} = 70.8 ppm. This is more lowfield shifted than in $(PhC)_4$BCl (δ_{11B} = 66.4 ppm) and $(Ph^FC)_4$B–Br (δ_{11B} = 67 ppm). Saito's structurally related example of 1-F-2,5-$(SiMe_2t\text{-}Bu)_2$-3,4-(Ph_2)-borole (**A**), however, features an ^{11}B-NMR resonance at δ_{11B} = 54.9 ppm in line with a pronounced B–F π-interaction.

To explore the synthetic potential of chloroborole **8**, we probed the accessibility of boroles by salt-metathesis approaches starting from **8** (Scheme 6). When $(Ph^*Li)_n$,

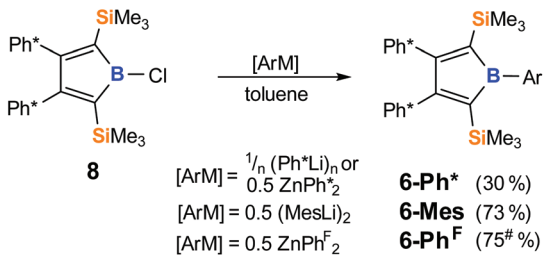

Scheme 6 Formation of **6-Ar** from **8** (yields after crystallization). #Repeatedly recrystallised product contained *ca.* 5–10% of an impurity that could not be separated.

Open Access Article. Published on 06 February 2020. Downloaded on 12/7/2025 11:21:56 AM.
This article is licensed under a Creative Commons Attribution-NonCommercial 3.0 Unported Licence.

$(MesLi)_2$ or $Zn(Ph^F)_2$ are added to toluene solutions of **8**, NMR monitoring indicates the crudes to primarily contain the respective aryl boroles **6-Ar** (>80%), however for **6-Ph*** and **6-Ph^F** isolated crystalline yields were lower. Notably, attempts to obtain **6-Ph** from this approach with PhLi or Ph_2Zn in toluene failed and gave intractable product mixtures, that contained intensely colored side products. An intensely green side product (<1% NMR) of unknown constitution was also observed in case of **6-Ph*** when prepared *via* the Ph*Li route. Only reactions of **8** with 0.5 equiv. $MgPh_2$ in THF led to clean formation of **6-Ph** which was again contaminated by THF. X-ray structures were obtained for **6-Ar** (Ar = Ph*, Mes, Ph^F) (Fig. 4). Crystals of **6-Ph** were repeatedly found to be thin needles that diffracted poorly. Comparable bond lengths within the central C_4B ring of all boroles **6-Ar** are virtually identical and are well in the range of Erker's related 1-Ph-2,5-disilylborole (**B-Ph**, Scheme 1)[82] and pentaaryl boroles[34,54,84] (except for $(PhC)_4BPh$ **D**).[1]

As observed for chloroborole **8**, in all cases the silyl-groups, and in some cases but much less pronounced C_β–Ph*, bend out of the central C_4B-plane by 9–15°. Even for aryls (such as Ph or Ph*) that do not feature substituents in *ortho*-position that would directly govern this torsion angle, the boron-bound aryls reveal rather large torsion angles between the respective C_4B- and aryl-planes of >50°. This is likely owing to the bulky silyl groups. With pentaaryl boroles, this torsion angle usually lies between 15–30°. The torsion of the C_β-bound aryls is much less affected. For **6-Ar** these torsions are found between 52–58° not much different from the torsions in $(PhC)_4BAr$ (45–55°)[1,34] or $(Ph*C)_4B$–Ar (52–58°).[84]

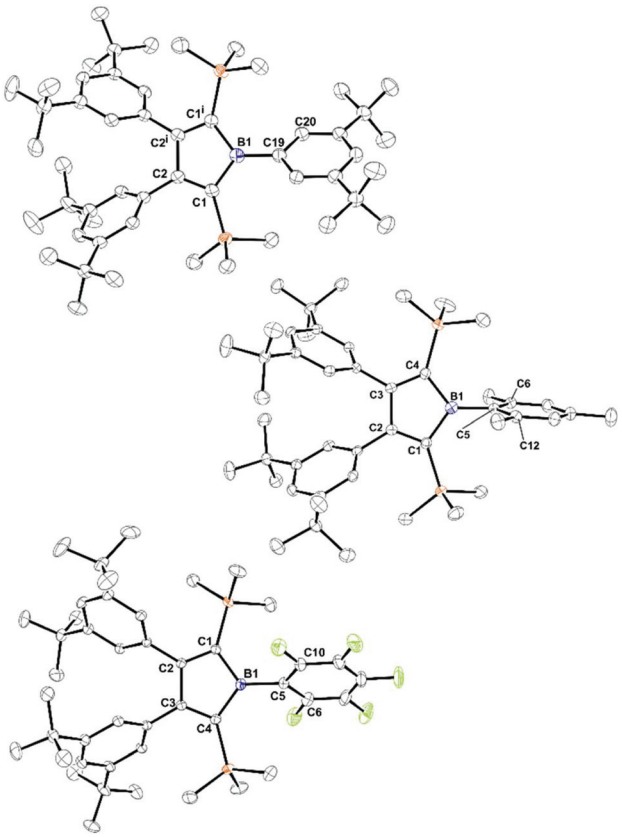

Fig. 4 ORTEP plots of the solid-state structure of boroles (**6-Ar**). Anisotropic displacement parameters are drawn at 50% probability level. Lattice solvent molecules and disordered *t*-Bu groups are omitted for the sake of clarity. Top: **6-Ph***, middle: **6-Mes**, bottom: **6-Ph^F**. Key structural features are summarized in Table 1.

The ^{11}B-NMR resonances in **6-Ar** are found at comparatively low field (Ar = Ph: 76.6 ppm; = Ph*: 77.1 ppm; = Mes: 79.9 ppm; = Ph^F: 77.4 ppm). Pentaaryl boroles ^{11}B resonances are usually found between 65 and 75 ppm (ref. 1, 30, 54 and 84) and Erker's **B-Ph** (Scheme 1) at 74.7 ppm.[82] Previously, only sterically congested mesityl substituted $(ArC)_4BMes$ boroles revealed ^{11}B resonances that low-field shifted (Ar = Ph: 79 ppm; Ar = thienyl: 77 ppm) indicating, that increasing perpendicularity of the B-bound aryl correlates with low-field shifts.

Properties of 2,5-disilylboroles

NICS[101–103] values for **6-Ar** and **8** were calculated and NICS(0) and NICS(1) are tabulated in Table 1. The impact of the 2,5-disilyl substitution pattern on the (anti)aromaticity of boroles causes the NICS(0) values to be lower than the parent **E** (20.6), but higher (with a maximum of 16.7 for **6-Ph^F**) than **D** $(PhC)_4BPh$ (13.6). However the NICS-profiles of **6-Ar** drop steeper and NICS(1) values do not differ significantly from **D** (see ESI†). The Lewis acidity of 2,5-disilylboroles was probed by means of the Gutmann–Beckett approach that correlates the ^{31}P chemical shift of $Et_3P{=}O$ interacting with Lewis acids with their acidity.[104–106] For steric reasons the Lewis-acidity of **6-Mes** is poorly accounted for by this method but **8** (70.7), **6-Ph*** (72.1), **6-Ph** (72.1) and even **6-Ph^F** (73.8) all reveal similar acceptor numbers (AN) well below those previously determined under identical conditions for **D** (78.7).[100] The bulky and electropositive silyl groups seem to lower the Lewis-acidity, however the method cannot provide insight which influence is dominating.

Since the isolation of deeply-blue $(PhC)_4BPh$ (λ_{max} 560 nm),[5] a striking feature of the hitherto well-characterized examples of pentaaryl boroles is their intense color with broad absorptions in the visible spectra roughly spanning from λ_{max} 530 nm (purple $(Ph^FC)_4BPh^F$)[54] to 635 nm (green $(PhC)_4BPh^F$).[30] Substitution with heteroaryls (*e.g.* thiophene) allowed even stronger shifts of λ_{max}.[53,60] The 2,5-disilyl-substituted boroles reported here are all orange to red both in solid state and in solution with absorption bands around 470 nm. We originally anticipated that having electropositive substituents, such as the $SiMe_3$ group, attached to the C_α-carbons in boroles should narrow the π/π^* gap, which is dominatingly responsible for the intense colorization, and thus induce a red-shifted absorption. However, the opposite seems to be the case. We therefore computationally probed the photochemical properties of the elusive parent borole $(HC)_4BH$ (**E**), the 2,5-disilyl-boroles **6-Ar** and pentaphenyl borole $(PhC)_4BPh$ (**D**) (Fig. 5).

This journal is © The Royal Society of Chemistry 2020

Open Access Article. Published on 06 February 2020. Downloaded on 12/7/2025 11:21:56 AM.
This article is licensed under a Creative Commons Attribution-NonCommercial 3.0 Unported Licence.

Table 1 Structural, spectroscopic and computational details of 2,5-$(SiMe_3)_2$-boroles and some references

Entry	B–C_α, C_α–C_β, C_β–C_β [a]	C_4B–Ar torsion[b]	δ ^{13}C (C_α, C_β)[c]	δ ^{11}B[c]	λ_{exp},[d] (λ_{calc}),[e] ε_λ[f]	HOMO/ LUMO/gap[g]	NICS[h]	δ ^{31}P[i] AN
8 chloroborole	1.568(2), 1.353(2), 1.538(2) 1.564(2), 1.354(2)	—	134.8, 182.1	70.8	447, (450) 258	−5.33/−3.55 1.78	14.0 6.5	73.0 70.7
6-Ph	—	—	139.2, 183.1	76.6	480, (475) —	−5.16/−3.50 1.66	15.1 7.4	73.6 72.1
6-Ph*	1.587(3), 1.355(3), 1.540(4)	51	139.2, 182.8	77.1	473, (469) 130	−5.11/−3.41 1.70	14.7 7.1	73.6 72.1
6-Mes	1.590(3), 1.360(4), 1.538(4) 1.594(4), 1.359(3)	85	138.8, 181.4	79.9	≈480, (462) 310	−5.17/−3.45 1.72	14.6 6.8	46.1 11.3
6-Ph^F	1.577(2), 1.359(2), 1.539 (2) 1.577(2), 1.357(2)	59	137.6, 184.8	77.4	≈505, (510) 121	−5.37/−3.83 1.54	16.7 8.4	74.4 73.8
D[1] $(PhC)_4BPh$	1.526(2), 1.428(2), 1.470(2) 1.539(2), 1.425(2)[j]	33	137.9, 162.1	65.4	560, (577)	−4.84/−3.64 1.20	13.6 7.2	76.6[100] 78.7
E $(HC)_4BH$	1.585, 1.348, 1.520[g]	—	—	—	—, (466)	−5.72/−3.95 1.77	20.6 11.5	—

[a] In [Å]. [b] Torsion angle in [°]. [c] In parts per million, ppm. [d] Absorption bands of lowest energy in nm. [e] TD-DFT: RIJCOSX-CAM-B3LYP\def2-SVP\ \RI-BP86-D3BJ\def2-TZVP. [f] In L mol^{-1} cm^{-1}. [g] RI-BP86\def2-TZVP, energies in eV. [h] $NICS_{iso}(0)$ and $NICS_{iso}(1)$ GIAO PBE0\def2-TZVP. [i] Gutmann–Beckett Lewis-acidity scale parameters derived from mixtures with Et_3PO in C_6D_6. Acceptor Numbers AN = 2.21 × (δ_{31P} −41). [j] Bond lengths as reported in ref. 1. Note that C_4B bond lengths in this structure markedly deviate from other known pentaaryl boroles.

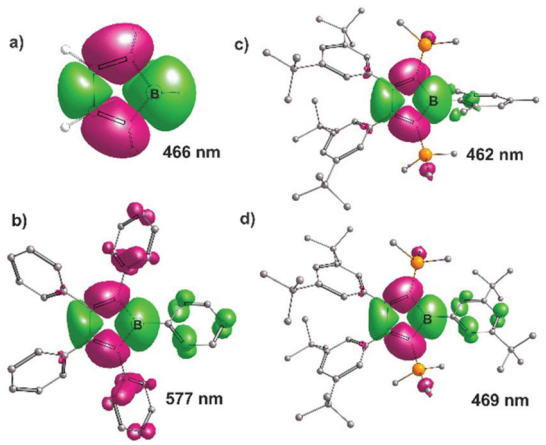

Fig. 5 Difference density plots for the computationally predicted lowest energy excitations of a series of boroles at an isovalue of 0.001 a. u.; (a) $(HC)_4BH$ **E**, (b) $(PhC)_4BPh$ **D**, (c) **6-Mes**, (d) **6-Ph*** (positive: green; negative: magenta). TD-DFT RIJCOSX-CAM-B3LYP\def2-SVP.

TD-DFT calculations on **8** and **6-Ar** reproduced the experimental absorption spectra very well. In all cases the lowest energy absorption is dominated by the π/π* transition between the borole C_4B based HOMO and LUMO. The absorption for the π/π* transition in parent $(HC)_4BH$ **E** is predicted at 466 nm well in the range where the respective resonances for **6-Ar** are found. The difference density plots for the respective excitations of **E** and **6-Mes** are very similar and highlight only minor contributions from substituents (Fig. 5).

Pentaphenylborole $(PhC)_4BPh$ however reveals major contributions both from the boron-bound (accepting) and C_α-bound (donating) phenyl π-systems. From comparison with our 2,5-disilylboroles we reason, that particularly the π-interaction of C_4B with C_α-bound aryls causes the red-shifted absorption that leads to the intense purple to green colors of (substituted) pentaphenyl boroles. Thus the 2,5-disilylboroles without perturbation of the C_4B π-system by arene ligands represent a much more accurate synthetic model of the parent, but elusive, $(HC)_4BH$ **E** when it comes to direct comparisons of the frontier orbital situation. This is also reflected in the HOMO–LUMO energies (Table 1).

To shed further light on the influence of aryl π-system interaction in boroles, in a qualitative computational approach, we probed the individual influence of C_4B bound aryls on the computationally predicted π/π* absorption band (Fig. 6).

Starting from a hypothetical structure of $(PhC)_4BPh$ with all phenyl groups perpendicular to the C_4B plane, TD-DFT predicts the absorption at 504 nm. Minimizing effective π-interaction thus apparently results in blueshifted absorptions closer to unperturbed $(HC)_4BH$ (**E**). From there on, gradually reducing the (C_4B)–Ph_i torsion angle at B-, C_α- and

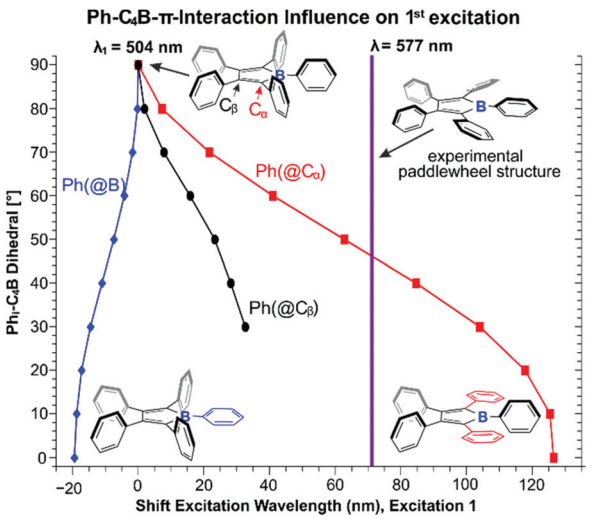

Fig. 6 TD-DFT predicted shifts in excitation wavelength of $(PhC)_4BPh$ depending on the torsion angle between C_4B-plane and B-bound, C_α-bound or C_β-bound phenyls.

Open Access Article. Published on 06 February 2020. Downloaded on 12/7/2025 11:21:56 AM.
This article is licensed under a Creative Commons Attribution-NonCommercial 3.0 Unported Licence.

(to a reduced extent due to eventual collapsing overlap) C_β-bound aryls to coplanarity allows a qualitative insight into the individual effects. While co-planarily bound B–Ph groups lead to only mildly blue-shifted absorptions likely due to a LUMO raise on account of more effective π-interaction, particularly co-planarily arranged C_α-bound phenyls reveal a strong red-shifting effect. This further corroborates the essential impact of C_α-bound aryls on the color and HOMO/LUMO gap of boroles that we identified from their substitution by silyl groups. The vast influence of the C_α aryl torsion may also be a reason for the broad bands ($\omega_{1/2} \approx 200$ nm) commonly observed for these transitions in pentaphenyl boroles. Some previous studies on heteroaryl substituted boroles already suggested the importance of torsion-angle dependent π-interaction affecting the spectroscopic features.[53,60]

Conclusion

In summary we presented various synthetic approaches to 2,5-disilyl boroles and shed light on their limitations. While traditional routes *via* boron-tin exchange reactions from stannoles fail, the reaction of the 1,4-dilithiobutadiene with aryl boron-dichlorides provides access to substituted boroles when the reaction is conducted in THF. In hydrocarbons two equivalents of aryl-boron dihalides react with 1,4-dilithiobutadienes to afford 2-boryl-3-borolenes, putatively *via* the free borole. Treatment of 1,4-dilithiobutadiene with BCl_3 grants access to a thermally robust chloroborole. The reactions of the chloroborole with common available aryl–carbon nucleophiles such as aryllithium, Grignard reagents and arylzinc reagents revealed to be very dependent on the substituent and often leads to colored product mixtures.

π/π*-absorption features of 2,5-disilyl-boroles are distinctive from pentaaryl boroles in that they do not reveal deeply blue colors. The differences were routed back to absence of π-interaction contributions stemming from C_α-bound aryl groups that are the foundation of the purple-to-blue color of pentaaryl boroles. Spectroscopically and regarding the frontier orbital situation, 2,5-disilylboroles are much closer to the parent, yet elusive borole $(HC)_4BH$. Given the field of free borole chemistry has been dominated by tetraphenyl-butadiene systems for 50 years, the new boroles and their access routes reported in this contribution represent a significant extension to the existing library of substitution patterns that allow the handling of free boroles. We are currently exploring the chemical potential of these boroles.

Experimental

Extensive synthetic and analytical details are given in the ESI.†

Conflicts of interest

Content of this manuscript is or will be included in the PhD/BSc theses of T. H. and L. N. There are no conflicts to declare.

Acknowledgements

Prof. Dietmar Stalke is most gratefully acknowledged for generous and supportive mentorship. We are grateful to the Fonds der chemischen Industrie for funding (fellowships to CPS and TH). The institute of inorganic chemistry is thanked for the provision of excellent conditions. We are grateful to LANXESS Organometallics GmbH for a chemical donation. MSc Paul Niklas Ruth is acknowledged for crystallographic advice and expertise. This contribution was funded by the Deutsche Forschungsgemeinschaft (DFG, German Research Foundation) - 389479699/GRK2455.

Notes and references

1 H. Braunschweig, I. Fernández, G. Frenking and T. Kupfer, *Angew. Chem., Int. Ed.*, 2008, **47**, 1951–1954.
2 H. Braunschweig and T. Kupfer, *Chem. Commun.*, 2008, **37**, 4487–4489.
3 H. Braunschweig, I. Krummenacher and J. Wahler, in *Advances in Organometallic Chemistry*, ed. A. F. Hill and M. J. Fink, Academic Press, 2013, vol. 61, pp. 1–53.
4 J. O. C. Jimenez-Halla, E. Matito, M. Sola, H. Braunschweig, C. Horl, I. Krummenacher and J. Wahler, *Dalton Trans.*, 2015, **44**, 6740–6747.
5 J. J. Eisch, N. K. Hota and S. Kozima, *J. Am. Chem. Soc.*, 1969, **91**, 4575–4577.
6 J. J. Eisch, J. E. Galle and S. Kozima, *J. Am. Chem. Soc.*, 1986, **108**, 379–385.
7 C. Fan, L. G. Mercier, W. E. Piers, H. M. Tuononen and M. Parvez, *J. Am. Chem. Soc.*, 2010, **132**, 9604–9606.
8 A. Y. Houghton, V. A. Karttunen, C. Fan, W. E. Piers and H. M. Tuononen, *J. Am. Chem. Soc.*, 2013, **135**, 941–947.
9 H. Braunschweig, A. Damme, C. Hörl, T. Kupfer and J. Wahler, *Organometallics*, 2013, **32**, 6800–6803.
10 B. C. Caputo, Z. J. Manning, J. H. Barnard and C. D. Martin, *Polyhedron*, 2016, **114**, 273–277.
11 A. Fukazawa, J. L. Dutton, C. Fan, L. G. Mercier, A. Y. Houghton, Q. Wu, W. E. Piers and M. Parvez, *Chem. Sci.*, 2012, **3**, 1814–1818.
12 H. Braunschweig, C.-W. Chiu, T. Kupfer and K. Radacki, *Inorg. Chem.*, 2011, **50**, 4247–4249.
13 K. Ansorg, H. Braunschweig, C. W. Chiu, B. Engels, D. Gamon, M. Hügel, T. Kupfer and K. Radacki, *Angew. Chem., Int. Ed.*, 2011, **50**, 2833–2836.
14 J. J. Eisch and J. E. Galle, *J. Am. Chem. Soc.*, 1975, **97**, 4436–4437.
15 J. J. Eisch, J. E. Galle, B. Shafii and A. L. Rheingold, *Organometallics*, 1990, **9**, 2342–2349.
16 S. A. Couchman, T. K. Thompson, D. J. D. Wilson, J. L. Dutton and C. D. Martin, *Chem. Commun.*, 2014, **50**, 11724–11726.
17 K. Huang, S. A. Couchman, D. J. D. Wilson, J. L. Dutton and C. D. Martin, *Inorg. Chem.*, 2015, **54**, 8957–8968.

This journal is © The Royal Society of Chemistry 2020

Open Access Article. Published on 06 February 2020. Downloaded on 12/7/2025 11:21:56 AM.
This article is licensed under a Creative Commons Attribution-NonCommercial 3.0 Unported Licence.

18 K. Huang and C. D. Martin, *Inorg. Chem.*, 2015, **54**, 1869–1875.
19 J. H. Barnard, S. Yruegas, K. Huang and C. D. Martin, *Chem. Commun.*, 2016, **52**, 9985–9991.
20 S. Yruegas, D. C. Patterson and C. D. Martin, *Chem. Commun.*, 2016, **52**, 6658–6661.
21 K. Huang and C. D. Martin, *Inorg. Chem.*, 2016, **55**, 330–337.
22 J. H. Barnard, S. Yruegas, S. A. Couchman, D. J. D. Wilson, J. L. Dutton and C. D. Martin, *Organometallics*, 2016, **35**, 929–931.
23 S. Yruegas and C. D. Martin, *Chem. – Eur. J.*, 2016, **22**, 18358–18361.
24 S. Yruegas, C. Wilson, J. L. Dutton and C. D. Martin, *Organometallics*, 2017, **36**, 2581–2587.
25 J. J. Baker, K. H. M. Al-Furaiji, O. T. Liyanage, D. J. D. Wilson, J. L. Dutton and C. D. Martin, *Chem. – Eur. J.*, 2019, **25**, 1581–1587.
26 H. Braunschweig, C. Hörl, L. Mailänder, K. Radacki and J. Wahler, *Chem. – Eur. J.*, 2014, **20**, 9858–9861.
27 H. Braunschweig, F. Hupp, I. Krummenacher, L. Mailänder and F. Rauch, *Chem. – Eur. J.*, 2015, **21**, 17844–17849.
28 H. Braunschweig, I. Krummenacher, L. Mailänder and F. Rauch, *Chem. Commun.*, 2015, **51**, 14513–14515.
29 H. Braunschweig, M. A. Celik, F. Hupp, I. Krummenacher and L. Mailänder, *Angew. Chem., Int. Ed.*, 2015, **54**, 6347–6351.
30 H. Braunschweig, M. A. Celik, T. Dellermann, G. Frenking, K. Hammond, F. Hupp, H. Kelch, I. Krummenacher, F. Lindl, L. Mailänder, J. H. Müssig and A. Ruppert, *Chem. – Eur. J.*, 2017, **23**, 8006–8013.
31 F. Lindl, S. Lin, I. Krummenacher, C. Lenczyk, A. Stoy, M. Müller, Z. Lin and H. Braunschweig, *Angew. Chem., Int. Ed.*, 2019, **58**, 338–342.
32 G. E. Herberich, B. Buller, B. Hessner and W. Oschmann, *J. Organomet. Chem.*, 1980, **195**, 253–259.
33 H. Braunschweig, C.-W. Chiu, A. Damme, B. Engels, D. Gamon, C. Hörl, T. Kupfer, I. Krummenacher, K. Radacki and C. Walter, *Chem. – Eur. J.*, 2012, **18**, 14292–14304.
34 C.-W. So, D. Watanabe, A. Wakamiya and S. Yamaguchi, *Organometallics*, 2008, **27**, 3496–3501.
35 H. Braunschweig and I. Krummenacher, in *Organic Redox Systems*, 2015, pp. 503–522, DOI: 10.1002/9781118858981.ch17.
36 G. E. Herberich, J. Hengesbach, U. Kölle, G. Huttner and A. Frank, *Angew. Chem., Int. Ed. Engl.*, 1976, **15**, 433–434.
37 G. E. Herberich, J. Hengesbach, U. Kölle and W. Oschmann, *Angew. Chem., Int. Ed. Engl.*, 1977, **16**, 42–43.
38 G. E. Herberich, B. Hessner, W. Boveleth, H. Lüthe, R. Saive and L. Zelenka, *Angew. Chem., Int. Ed. Engl.*, 1983, **22**, 996–996.
39 G. E. Herberich, W. Boveleth, B. Hessner, D. P. J. Köffer, M. Negele and R. Saive, *J. Organomet. Chem.*, 1986, **308**, 153–166.
40 G. E. Herberich, B. Hessner, H. Ohst and I. A. Raap, *J. Organomet. Chem.*, 1988, **348**, 305–316.
41 G. E. Herberich, U. Englert, M. Hostalek and R. Laven, *Chem. Ber.*, 1991, **124**, 17–23.
42 G. E. Herberich, T. Carstensen and U. Englert, *Chem. Ber.*, 1992, **125**, 2351–2357.
43 R. W. Quan, G. C. Bazan, W. P. Schaefer, J. E. Bercaw and A. F. Kiely, *J. Am. Chem. Soc.*, 1994, **116**, 4489–4490.
44 C. K. Sperry, W. D. Cotter, R. A. Lee, R. J. Lachicotte and G. C. Bazan, *J. Am. Chem. Soc.*, 1998, **120**, 7791–7805.
45 G. J. Pindado, S. J. Lancaster, M. Thornton-Pett and M. Bochmann, *J. Am. Chem. Soc.*, 1998, **120**, 6816–6817.
46 T. J. Woodman, M. Thornton-Pett, D. L. Hughes and M. Bochmann, *Organometallics*, 2001, **20**, 4080–4091.
47 P. Tholen, Z. Dong, M. Schmidtmann, L. Albers and T. Müller, *Angew. Chem., Int. Ed.*, 2018, **57**, 13319–13324.
48 C. P. Sindlinger and P. N. Ruth, *Angew. Chem., Int. Ed.*, 2019, **58**, 15051–15056.
49 P. J. Fagan, E. G. Burns and J. C. Calabrese, *J. Am. Chem. Soc.*, 1988, **110**, 2979–2981.
50 X. Su, J. J. Baker and C. D. Martin, *Chem. Sci.*, 2020, **11**, 126–131.
51 J. J. Baker, K. H. M. Al Furaiji, O. T. Liyanage, D. J. D. Wilson, J. L. Dutton and C. D. Martin, *Chem. – Eur. J.*, 2019, **25**, 1581–1587.
52 This discussion does not include systems where the borole 4π-electron system is embedded in larger, delocalised aromatic framworks as for example in 9-borafluorenes.
53 T. Araki, A. Fukazawa and S. Yamaguchi, *Angew. Chem., Int. Ed.*, 2012, **51**, 5484–5487.
54 C. Fan, W. E. Piers and M. Parvez, *Angew. Chem., Int. Ed.*, 2009, **48**, 2955–2958.
55 H. Braunschweig, C.-W. Chiu, J. Wahler, K. Radacki and T. Kupfer, *Chem. – Eur. J.*, 2010, **16**, 12229–12233.
56 H. Braunschweig, C.-W. Chiu, K. Radacki and P. Brenner, *Chem. Commun.*, 2010, **46**, 916–918.
57 H. Braunschweig, C.-W. Chiu, A. Damme, K. Ferkinghoff, K. Kraft, K. Radacki and J. Wahler, *Organometallics*, 2011, **30**, 3210–3216.
58 H. Braunschweig, V. Dyakonov, J. O. C. Jimenez-Halla, K. Kraft, I. Krummenacher, K. Radacki, A. Sperlich and J. Wahler, *Angew. Chem., Int. Ed.*, 2012, **51**, 2977–2980.
59 H. Braunschweig, C.-W. Chiu, D. Gamon, M. Kaupp, I. Krummenacher, T. Kupfer, R. Müller and K. Radacki, *Chem. – Eur. J.*, 2012, **18**, 11732–11746.
60 H. Braunschweig, A. Damme, J. O. C. Jimenez-Halla, C. Hörl, I. Krummenacher, T. Kupfer, L. Mailänder and K. Radacki, *J. Am. Chem. Soc.*, 2012, **134**, 20169–20177.
61 A. J. Ashe, J. W. Kampf and P. M. Savla, *Organometallics*, 1993, **12**, 3350–3353.
62 L. Liu, W.-X. Zhang, Q. Luo, H. Li and Z. Xi, *Organometallics*, 2010, **29**, 278–281.
63 S. Zhang, M. Zhan, W.-X. Zhang and Z. Xi, *Organometallics*, 2013, **32**, 4020–4023.

Open Access Article. Published on 06 February 2020. Downloaded on 12/7/2025 11:21:56 AM.
This article is licensed under a Creative Commons Attribution-NonCommercial 3.0 Unported Licence.

64 J. Wei, L. Liu, M. Zhan, L. Xu, W.-X. Zhang and Z. Xi, *Angew. Chem., Int. Ed.*, 2014, **53**, 5634–5638.
65 Y. Zhang, J. Wei, W.-X. Zhang and Z. Xi, *Inorg. Chem.*, 2015, **54**, 10695–10700.
66 Y. Zhang, Y. Chi, J. Wei, Q. Yang, Z. Yang, H. Chen, R. Yang, W.-X. Zhang and Z. Xi, *Organometallics*, 2017, **36**, 2982–2986.
67 B. Wei, L. Liu, W.-X. Zhang and Z. Xi, *Angew. Chem., Int. Ed.*, 2017, **56**, 9188–9192.
68 Y. Zhang, Z. Yang, W.-X. Zhang and Z. Xi, *Chem. – Eur. J.*, 2019, **25**, 4218–4224.
69 M. Saito, T. Akiba, M. Kaneko, T. Kawamura, M. Abe, M. Hada and M. Minoura, *Chem. – Eur. J.*, 2013, **19**, 16946–16953.
70 T. Kuwabara, J.-D. Guo, S. Nagase, T. Sasamori, N. Tokitoh and M. Saito, *J. Am. Chem. Soc.*, 2014, **136**, 13059–13064.
71 T. Kuwabara, J.-D. Guo, S. Nagase, M. Minoura, R. H. Herber and M. Saito, *Organometallics*, 2014, **33**, 2910–2913.
72 T. Kuwabara and M. Saito, *Organometallics*, 2015, **34**, 4202–4204.
73 M. Nakada, T. Kuwabara, S. Furukawa, M. Hada, M. Minoura and M. Saito, *Chem. Sci.*, 2017, **8**, 3092–3097.
74 M. Saito, T. Akiba, S. Furukawa, M. Minoura, M. Hada and H. Y. Yoshikawa, *Organometallics*, 2017, **36**, 2487–2490.
75 Z. Dong, C. R. W. Reinhold, M. Schmidtmann and T. Müller, *J. Am. Chem. Soc.*, 2017, **139**, 7117–7123.
76 Z. Dong, O. Janka, J. Kösters, M. Schmidtmann and T. Müller, *Angew. Chem., Int. Ed.*, 2018, **57**, 8634–8638.
77 Z. Dong, C. R. W. Reinhold, M. Schmidtmann and T. Müller, *Organometallics*, 2018, **37**, 4736–4743.
78 Z. Dong, M. Schmidtmann and T. Müller, *Z. Anorg. Allg. Chem.*, 2018, **644**, 1041–1046.
79 C. R. W. Reinhold, Z. Dong, J. M. Winkler, H. Steinert, M. Schmidtmann and T. Müller, *Chem. – Eur. J.*, 2018, **24**, 848–854.
80 Z. Dong, M. Schmidtmann and T. Müller, *Chem. – Eur. J.*, 2019, **25**, 10858–10865.
81 Z. Dong, L. Albers, M. Schmidtmann and T. Müller, *Chem. – Eur. J.*, 2019, **25**, 1098–1105.
82 F. Ge, G. Kehr, C. G. Daniliuc and G. Erker, *J. Am. Chem. Soc.*, 2014, **136**, 68–71.
83 V. Y. Lee, H. Sugasawa, O. A. Gapurenko, R. M. Minyaev, V. I. Minkin, H. Gornitzka and A. Sekiguchi, *J. Am. Chem. Soc.*, 2018, **140**, 6053–6056.
84 T. Heitkemper and C. P. Sindlinger, *Chem. – Eur. J.*, 2019, **25**, 6628–6637.
85 X. Yan and C. Xi, *Acc. Chem. Res.*, 2015, **48**, 935–946.
86 P. J. Fagan and W. A. Nugent, *J. Am. Chem. Soc.*, 1988, **110**, 2310–2312.
87 P. J. Fagan, W. A. Nugent and J. C. Calabrese, *J. Am. Chem. Soc.*, 1994, **116**, 1880–1889.
88 M. Saito, M. Nakamura, T. Tajima and M. Yoshioka, *Angew. Chem., Int. Ed.*, 2007, **46**, 1504–1507.
89 E.-I. Negishi and T. Takahashi, *Acc. Chem. Res.*, 1994, **27**, 124–130.
90 U. Rosenthal, A. Ohff, W. Baumann, A. Tillack, H. Görls, V. V. Burlakov and V. B. Shur, *Z. Anorg. Allg. Chem.*, 1995, **621**, 77–83.
91 A. D. Miller, J. F. Tannaci, S. A. Johnson, H. Lee, J. L. McBee and T. D. Tilley, *J. Am. Chem. Soc.*, 2009, **131**, 4917–4927.
92 C. Xi, S. Huo, T. H. Afifi, R. Hara and T. Takahashi, *Tetrahedron Lett.*, 1997, **38**, 4099–4102.
93 The crystal structure of **4** is documented in the ESI.†
94 C. Wang, Q. Luo, H. Sun, X. Guo and Z. Xi, *J. Am. Chem. Soc.*, 2007, **129**, 3094–3095.
95 Q. Luo, C. Wang, L. Gu, W.-X. Zhang and Z. Xi, *Chem. – Asian J.*, 2010, **5**, 1120–1128.
96 Analytical and crystallographic data for **5** is documented in the ESI.†
97 H. Braunschweig, M. Dömling, S. Kachel, H. Kelch, T. Kramer, I. Krummenacher, C. Lenczyk, S. Lin, Z. Lin, C. Possiel and K. Radacki, *Chem. – Eur. J.*, 2017, **23**, 16167–16170.
98 V. A. K. Adiraju and C. D. Martin, *Chem. – Eur. J.*, 2017, **23**, 11437–11444.
99 Z. Zhang, Z. Wang, M. Haehnel, A. Eichhorn, R. M. Edkins, A. Steffen, A. Krueger, Z. Lin and T. B. Marder, *Chem. Commun.*, 2016, **52**, 9707–9710.
100 S. Yruegas, J. J. Martinez and C. D. Martin, *Chem. Commun.*, 2018, **54**, 6808–6811.
101 P. V. R. Schleyer, C. Maerker, A. Dransfeld, H. Jiao and N. J. R. van Eikema Hommes, *J. Am. Chem. Soc.*, 1996, **118**, 6317–6318.
102 Z. Chen, C. S. Wannere, C. Corminboeuf, R. Puchta and P. V. R. Schleyer, *Chem. Rev.*, 2005, **105**, 3842–3888.
103 A. Stanger, *J. Org. Chem.*, 2006, **71**, 883–893.
104 U. Mayer, V. Gutmann and W. Gerger, *Monatsh. Chem.*, 1975, **106**, 1235–1257.
105 M. A. Beckett, G. C. Strickland, J. R. Holland and K. Sukumar Varma, *Polymer*, 1996, **37**, 4629–4631.
106 I. B. Sivaev and V. I. Bregadze, *Coord. Chem. Rev.*, 2014, **270–271**, 75–88.

This journal is © The Royal Society of Chemistry 2020